Lawrence Berkeley National Laboratory
Advanced Light Source

Title
Surface slope metrology of highly curved x-ray optics with an interferometric microscope

Permalink
https://escholarship.org/uc/item/1sm4t2w6

ISBN
978-1-5106-1227-3

Authors
Gevorkyan, Gevork S
Centers, Gary
Polonska, Kateryna S
et al.

Publication Date
2017-09-07

DOI
10.1117/12.2274220

Peer reviewed

eScholarship.org Powered by the California Digital Library
University of California

Surface slope metrology of highly curved x-ray optics with an interferometric microscope

Gevork S. Gevorkyan*[a], Gary Centers [a,b], Kateryna S. Polonska[a,c], Sergey M. Nikitin[a], Ian Lacey[a], Valeriy V. Yashchuk[a]

[a]Lawrence Berkeley National Laboratory, Advanced Light Source, One Cyclotron Road, Berkeley, CA, USA 94720; [b]Helmholtz Institute, JGU Mainz, Staudingerweg 18, Mainz, Germany 55128; [c]Physical, Technical and Computer Sciences Institute of Yuriy Fedkovich Chernivtsi National University, 2 Kotsjubynskyi Str., Chernivtsi, Ukraine 58012

ABSTRACT

The development of deterministic polishing techniques has given rise to vendors that manufacture high quality three-dimensional x-ray optics. The surface metrology on these optics remains a difficult task. For the fabrication, vendors usually use unique surface metrology tools, generally developed on site, that are not available in the optical metrology labs at x-ray facilities. At the Advanced Light Source X-Ray Optics Laboratory, we have developed a rather straightforward interferometric-microscopy-based procedure capable of sub microradian characterization of sagittal slope variation of x-ray optics for two-dimensionally focusing and collimating (such as ellipsoids, paraboloids, etc.). In the paper, we provide the mathematical foundation of the procedure and describe the related instrument calibration. We also present analytical expression describing the ideal surface shape in the sagittal direction of a spheroid specified by the conjugate parameters of the optic's beamline application. The expression is useful when analyzing data obtained with such optics. The high efficiency of the developed measurement and data analysis procedures is demonstrated in results of measurements with a number of x-ray optics with sagittal radius of curvature between 56 mm and 480 mm. We also discuss potential areas of further improvement.

Keywords: x-ray optics, high curvature mirrors, optical metrology, precision surface measurements, interferometric microscopy, calibration, residual slope variation

1. INTRODUCTION

The advances in polishing technology have given rise to 3D optics for x-ray applications. Using deterministic polishing techniques, vendors are able to produce synchrotron grade x-ray mirrors, e.g. in the shape of a toroid, an ellipsoid, or a hyperboloid. The specification of these optics is often given in the slope domain for the optic's tangential and sagittal directions. There is a typical forgiveness factor, proportional to the grazing incidence angle of light, which makes the sagittal axis specification of the optic less stringent than the tangential axis.

The Advanced Light Source (ALS) X-ray Optics Laboratory (XROL)[1,2] has two surface slope profilers, the Long Trace Profiler (LTP-II)[3,4], and the Developmental Long Trace Profiler (DLTP)[5,6] designed in-house on an autocollimator and moving mirror-based pentaprism[7,8] schematic similar to HZB/BESSY-II NOM.[9,10] The LTP-II has a precision of down to ~0.2 µrad (root-mean-square, rms),[3,4] but measurements of optics beyond ~10 m ROC are not plausible using a pencil beam interferometer based slope profiler.[11,12] The DLTP has a slope measuring precision of on the level of ~0.1 µrad (rms),[3,4] but also cannot measure curved optics with ROC below ~10 m. This problem exists in general for NOM-like systems.[13-15] The surface slope measuring tools of these types cannot produce sensible slope measurement results for significantly curved optics such as three dimensional (3D) x-ray mirrors with typical sagittal curvature <<10 meters.

A method for characterizing the figure of a significantly curved optic was developed by the group of Kazuto Yamauchi at Osaka University. The method involves sequential height measurements over overlapped sub-areas with an interferometric microscope and stitching the measurements (micro stitching interferometry, MSI). The mutual alignment of the sub-areas used for stitching is based on a lower resolution profile of the entire area obtained with a large field of view Fizeau interferometer using relative angle determinable stitching interferometry (RADSI) method.[17-19] The RADSI/MSI system is unique proprietary metrology tool and currently is not available to metrology labs at x-ray

*Ggevorkyan@lbl.gov; phone 1 510 495-2592; lbl.gov

facilities outside Japan. Transfer of these technologies to JTEC Corporation (Japan) has made the company the sole world leader in the x-ray optics fabrication industry. Now, unprecedented ultra-precision x-ray optics are commercially available from the company. With such high quality x-ray focusing elliptically-shaped KB mirrors, with surface slope errors of about 30 nrad (rms), the two-dimensional diffraction-limited focusing of hard x-rays with a record focal spot size of about 7-8 nm has been obtained at the SPring-8/RIKEN.[20]

As a relatively simple way of measuring residual slope variation of significantly curved optics with an interferometric microscope, we discuss here using a method that can be thought as a curvature stitching technique. Using the curvature transform to residual slope (CTRS) measurement technique described in this article, we can characterize the residual slope variation in the sagittal direction of sagittally curved 3D x-ray optics. The CTRS method takes a local curvature trace along the sagittal direction of a high curvature optic and produces the residual slope variation along that trace. This does not need a tool such as RADSI for mutual alignment of the sub-areas measured with the interferometric microscope because we do stitching in the curvature domain, rather than in the height or slope domain. Therefore, relative tilt of the sub-areas does not come in to the problem. This method avoids problems of height and tilt uncertainty, both of which are being negated to first approximation when dealing with data in the curvature domain.

In this article, we discuss the theoretical basis of this curvature stitching method, and we overview different approaches to numerical integration of curvature. We describe the measurement apparatus and the steps taken to properly calibrate the instrument for reliable local curvature detrendings. We apply this method to tree optics, high sagittal curvature 3D toroid cylindrical mirror being transparent glass. We also apply this method to an ellipsoidal optic where we compare measured results to the analytical expressions for a mirror with the shape of an ellipsoid of revolution defined via the set of the conjugate parameters given by the mirror beamline (BL) application.

2. OBTAINING RESIDUAL SLOPE FROM LOCAL CURVATURE TRACES

2.1 Theory of CTRS, obtaining residual slope through numerical integration of curvature

Given a surface height distribution $h(x)$, it is common practice to convert to the first and second derivatives to represent slope and curvature:

$$h'(x) = \alpha(x) \tag{1}$$

$$C(x) = \frac{|h''|}{(1+h')^{\frac{3}{2}}} \tag{2}$$

What has not been commonly done, and is proposed here, is to start from a distribution of local curvature values and calculate the corresponding slope variation.[8] Since our curvature data will be a set of discrete points recorded with an increment Δx, we can use simple stepwise sum numerical integration method to acquire slope. The assumption used here is that the slope is small compared with unity:

$$C(x) \approx \left|\frac{d^2h}{dx^2}\right| \quad \text{for} \quad h' \ll 1 \tag{3}$$

$$\alpha(x_i) = \Delta x \sum_{j=1}^{i} C(x_j) \tag{4}$$

The issue with this integrated slope value is that the initial $\alpha(0)$ value is unknown, and in practice we just used 0 for the first value in the stepwise sum. The slopes found through this method are effectively detrended using a linear fitting of the average curvature, $\hat{C}$, and therefore correspond to the residual slope trace of the measured optic:

$$\Delta C(x_j) = C(x_j) - \frac{1}{N}\sum_{j=1}^{N} C(x_j) = C(x_j) - \hat{C} \tag{5}$$

$$\Delta\alpha(x_i) = \Delta x \sum_{j=1}^{i} \Delta C(x_j) \tag{6}$$

This stepwise sum is one of many methods to produce a discrete numerical integral. This method has a well-known problem of accumulative error when integrating experimental data with a random error. A more effective numerical integration technical, the trapezoidal rule, is used below. Others have discussed eliminating the issue of weighting on numerical integrals using discrete Fourier transform based numerical integration.[21] For the purpose of consistency in all demonstrations of the CTRS method, we used the trapezoidal method due to its simplicity.

2.2 ZYGO NewView interferometric microscope

The tool used to implement the CTRS method was the ZYGO NewView^{TM}-7300 interferometric microscope (Fig. 1) equipped for the measurements discussed throughout this paper with a 2.5x objective and a 1x zoom lens. We are permanently working to improve performance of this instrument, and it currently provides surface height data with a sub-angstrom precision.[22] The instrument was calibrated to improve the accuracy of measurements through the suppression of contributions from noise and from systematic errors such as objective lens aberrations.[23]

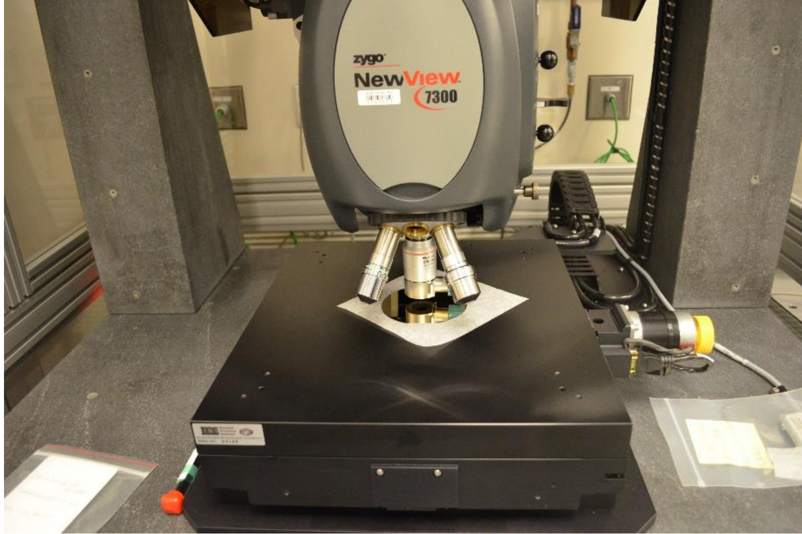

Figure 1. ZYGO NewView interferometric microscope sitting in closed hatches on a custom made granite table at the ALS XROL cleanroom.[1,2]

Because the CTRS method relies on accurate measurement of the surface radius of curvature with the ZYGO NewView interferometric microscope, we calibrated the microscope by measuring a number of spherical reference mirrors, purchased from Thorlabs, Inc., with 150 mm, 400 mm, and 1000 mm specified radius of curvatures. Preliminarily, the radii of all three mirrors were accurately measured using the radius measurement capability of the XROL ZYGO DynaFiz^{TM} interferometer. The calibration curves for X- and Y-directions of the microscope are shown in Fig. 2. The calibration factor for the NewView with 2.5× objective and 0.5× zoom, α, was determined to be constant and was derived using the nominal and measurement radii of the reference surfaces:

$$K_{\text{nominal}} = \alpha K_{\text{measured}} \tag{7}$$

Using Eq. (7) as a best fit model, we calibrated both the X-axis curvature and the X-axis curvature.[25]

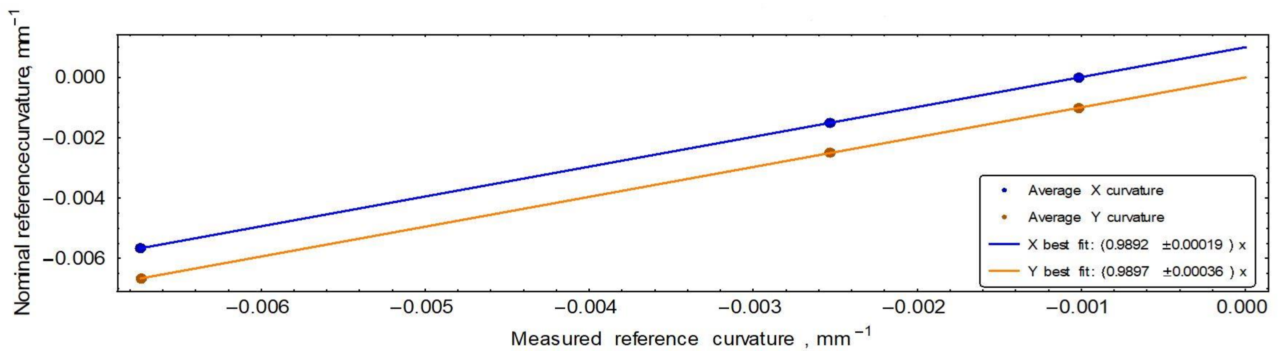

Figure 2. The calibration plot where each point corresponds to the measured curvature of each reference mirror in the X and Y directions of the NewView. The slope of the best fit line, seen in the plot's legend, passing through the origin determines the calibration factor. The X results are offset from Y by .001 for clarity.

Because the radius of surface curvature obtained in a single measurement with the microscope corresponds to an area of 1 mm^2, which is significantly smaller that the mask of 1 cm diameter used in the interferometric measurements, each curvature value used for the calibration was the average of three curvatures of independent locations within the center 1 cm diameter circle of the reference mirror surface. In order to minimize the contribution of the microscope aberration, a reference measurement taken with a super polished flat reference was subtracted from the profiles measured with the spherical mirrors. While accounting for a significant portion of the aberration error, this method is not absolute because of the dependence of the aberration on the SUT shape. Nevertheless, the limitation is acceptable in the case of measurement of the slope variation (through the curvature variation) of most of 3D x-ray mirrors because for any given mirror the variation of the curvature is usually small.

As the result of the discussed calibration of the NewView with 2.5× objective and 0.5× zoom, the best linear fit calibration factors are:

$$(\alpha_x, \alpha_y) = (0.9892, 0.9897) \quad (8)$$

These calibration scalers were used to adjust all CTRS method measurements. To best conduct each curvature trace while minimizing unwanted operator errors, we applied all measurements using a precision tracing scheme. There are some key elements which helps to reduce the operator error, one of those deals with the initial focus of the fringe patterns as seen from the microscope. Through testing, we have determined that starting at difference focus positions varying by as low as a single fringe will change the aberration error of the instrument (see also relevant discussion in Ref.[17]). To minimize the variation of the aberration error, in the course of measurements, we specially put efforts to adjust a distinct focus position applying a repeatable focusing process with the goal to use the same fringe pattern for each measurement (Fig. 3).

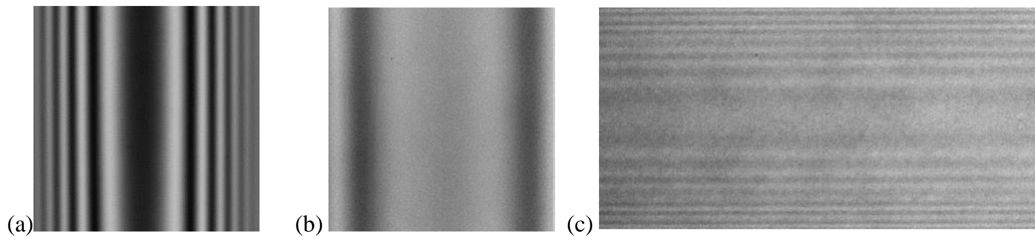

Figure 3. Interference fringe patterns of three optics[23-,25] with high sagittal curvature. All were measured with the CTRS method using a precision tracing scheme (see discussion in Secs. 3). We have a toroidal mirror (a) with 698 mm sagittal ROC, a cylindrical transparent glass substrate (b) with a 350 mm sagittal ROC, and an ellipsoidal mirror (c) with approximately a 55.8 mm sagittal ROC

Similarly, we prescribe a repeatable scheme for the microscope X-Y translation stage controls. After choosing the X-axis position, the location along the tangential direction which will be measured, we only shift along the Y-axis sagittal direction with the desired increment. Since the system has up to 4 digits of resolution, we are able to resolve the correct position on the surface of the optic down to ~0.1 µm. We are able to resolve the pitch and roll angular alignment for the microscope's optical head tilting stage down to ~2 µrad.

Each curvature trace is the average of two traces obtained with processing the measurements in forward (in the direction of increasing position value) and backward (in the direction of decreasing position value). This suppresses the instrumental drift error[26,27] and reduces error due to the subjective character of the focusing procedure discussed above. Note that the ZYGO NewView-7300 microscope is capable of automated repeatable measurements by translating the SUT and refocusing the optical head. However, the reliability of such automated measurements is questionable because of the high accuracy of instrument tuning required for each sub-area measurement. This same problem is seen in the automated stitching application of the microscope.

3. MEASURING HIGHLY CURVED OPTICS WITH THE ZYGO NEWVIEW

3.1 Toroidal x-ray mirror

As an example of the application of the CTRS method, we present here the residual slope variation results of a toroidal mirror with nominal radii 181 m in the tangential direction and 698 mm in the sagittal direction[24] for the ALS Polymer Scanning Transmission X-Ray Microscopy (STXM) beamline 5.3.2.2. Figure 4 shows the measurement arrangement.

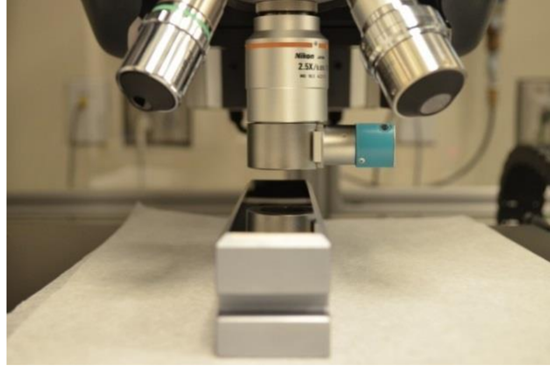

Figure 4. Toroidal mirror from BL 5.3.2.2 placed for measurements with the XROL ZYGO NewView-7300 interferometric microscope with scanning along X-axis of the microscope translation stage.

Figure 5 shows the residual slope variation in the sagittal direction of a 699 mm ROC toroidal mirror measured at the mirror tangential center. The trace is the average of two pairs of traces. Each pair contains scans carried out in opposite directions the mirror's sagittal direction. Additionally, in order to gain the reliability of the measurements, the mirror was rotated 90º CCW, swapping X-axis and Y-axis scanning translation of the stage and premeasured.

In order to get the trace in the slope domain (Fig. 5), the surface height distributions measured according to the CTRS method discibed above were cylindrically detrended with the instrumental software. The obtained curvatures after recalibration were transformed into the slope domain using the trapezoidal method of numerical integration. By averaging four slope values for each position measured on the optic's surface, we obtained the resulted averaged residual slope trace along the sagittal direction of the toroidal mirror.

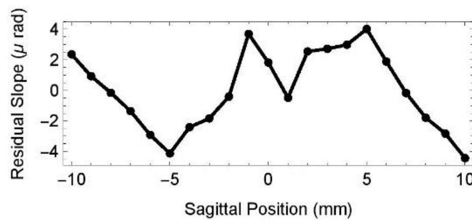

Figure 5. The residual slope variation in the sagittal direction of a 699 mm ROC toroidal mirror measured at the mirror tangential center. This is the average of four traces as discussed in the text.

The average ROC over the 20 mm clear aperture was 698.8 mm with a precision of 0.1 mm. The rms sagittal slope variation of the surface was 2.6 μrad, and that is well within the mirror specification.

A verification of the reliability of the repeatable retuning and realignment of the microscope in the course of the measurements, we also recorded the focus height as the microscope' optical head Z-axis position and the head pitch and roll alignment. These data are depicted in Fig. 6.

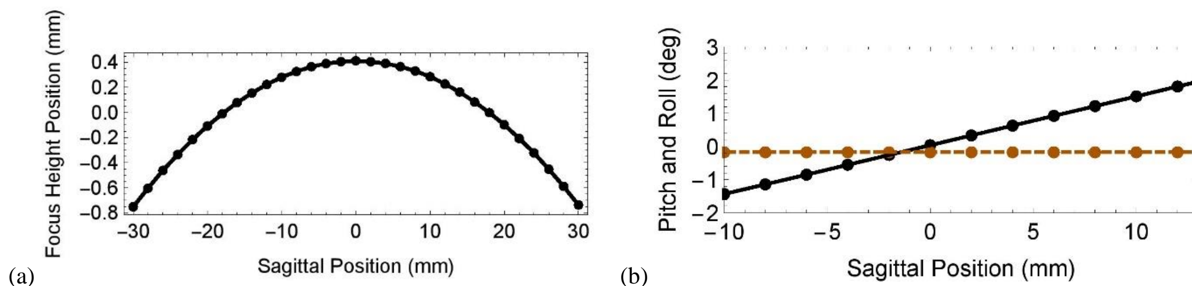

Figure 6. Focus height and angular alignment measurements for two CTRS traces for the BL 5.3.2.2 toroidal mirror. The focus height (a) and the constant pitch and increasing roll (b) alignments are shown for two traces on the same positions of the toroidal mirror. Swapping the x-axis and the y-axis with each other does will not effect the CTRS method if the instrument is properly calibrated.

The focus height and pitch variations in Fig. 6 correspond to the expectation for the cylindrical sagittal shape of the mirror. The smooth character of the variations and low random variation of the points suggest for the high reliability of the focusing and alignment procedure developed for the measurements.

Note that in Fig. 4, the microscope optical head is aligned to the mirror pole that appeared to be shifted from the mirror geometric shape by approximately 4.2 mm. The pole shift was verified by flipping the mirror and measuring the pitch (and roll) angular difference. The pole shift in the tangential direction was found to be more than 30 mm. The shift can be thought as a result of a misalignment of the bottom surface of the mirror substrate with respect to the mirror reflective surface.

3.2 Transparent glass cylindrical substrate

Measurements of transparent substrates are typically difficult because most types of surface slope metrology are reflection based. The NewView is capable of measuring transparent optics if back reflections don't interfere with surface reflection; if an optic is thick enough then the interference fringe patterns will not overlap and the focus scanning range of the microscope will only capture the surface of the optic.

Figure 7 depicts the arrangement of the NewView microscope set for measurement with a cylindrical mirror made of coated glass with the specified radius of curvature in the tangential direction of about 352 mm.[21]

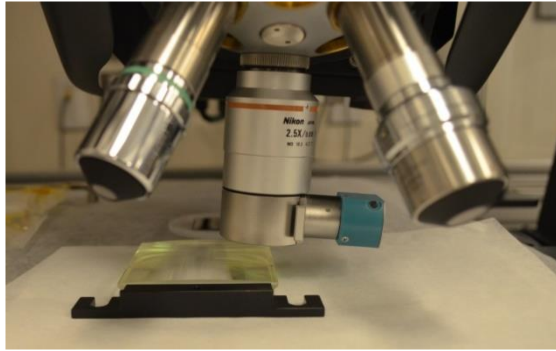

Figure 7. The arrangement of the NewView microscope set for measurement with a highly curved cylindrical mirror with the specified radius of curvature in the tangential direction of 352 mm.

The residual slope distributions measured along the tangential axis at the sagittal center of the mirror clear aperture is presented in Fig. 8. Both traces were measured over the same point on the mirror surface but two different operators and during two sequential days. The operators used the CTRS method for data acquisition and analysis. The coincidence of the results in Fig. 8 can be thought as a proof of the high reproducibility provided by the method with the uncertainty below 2 μrad (rms) found from the difference of the traces in Fig. 8.

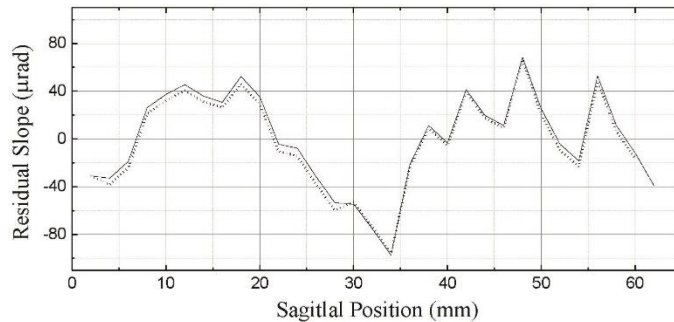

Figure 8. Residual slope distribution of the cylindrical glass substrate shown in Fig. 7. The two traces are shown as they were measured by to different operator with a day delay between the measurements. The average measured ROC over a 60 mm clear aperture was 352.2 mm, and the residual slope variation was 36.2 μrad (rms). The rms variation of the difference of the measurements is 2.47 μrad. The corresponding measurement uncertainty is $2.47/\sqrt{2} \approx 1.75$ μrad.

3.3 Ellipsoidal mirror

Another important type of substrate is 3D mirrors with the shape of an ellipsoid of revolution (spheroid, or 3D ellipsoidal mirror), and we used the CTRS method to measure the sagittal slope variation of one of them fabricated for the ALS Surface and Materials Science BL 8.0.1.

Figure 9 depicts the arrangement of the NewView microscope set for measurement with the 3D ellipsoid mirror.

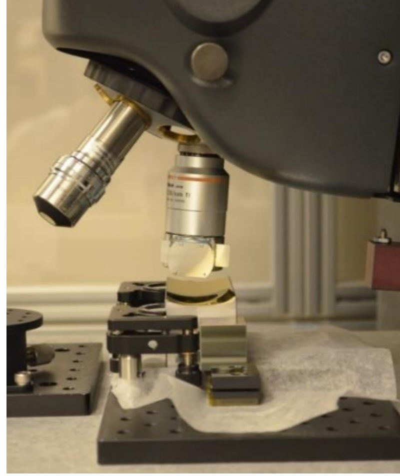

Figure 9. Mirror with the shape of an ellipsoid of revolution (spheroid) placed under ZYGO NewView™-7300 interferometric microscope available at the ALS XROL for characterization of sagittal slope variation in a few tangential positions.

The substrate is single crystal silicon with an overall size 100 mm (length in tangential direction) by 40 mm (width in sagittal direction) by 35 mm (height). The clear aperture is 80 mm x 20 mm, and the mirror is being used with the conjugate parameters[12] of distance from mirror center to the point source:

$$R_0 = 2.4 \text{ m} \tag{9}$$

the distance from the mirror center to the focus

$$R_0' = 1.2 \text{ m} \tag{10}$$

and the grazing incidence angle

$$\theta_0 = 2° \tag{11}$$

In order to compare the results of measurements with the ideal shape of the 3D ellipsoidal mirror, we derived a general equation describing the dependence of the sagittal radius of curvature $r_{SAG}(x)$ of the spheroid mirror on the tangential position x in the mirror coordinate system centered at the mirror pole (the details of the derivations can be found in Ref.[28]):

$$r_{sag}(x) = r_{sag,0}\sqrt{1 - \frac{\sqrt{(R_0+R_0')^2 - 4R_0R_0'\sin^2\theta_0}}{(R_0+R_0')R_0R_0'}|R_0 - R_0'|x - \frac{[(R_0+R_0')^2 - 4R_0R_0'\sin^2\theta_0]}{(R_0+R_0')^2R_0R_0'}x^2} \tag{12}$$

where $r_{sag,0}$ is the sagittal radius of curvature at the position of the mirror pole:

$$r_{sag,0} = 2\sin\theta\frac{R_0R_0'}{(R_0+R_0')} \tag{13}$$

For completeness, the Tangential radius of curvature at the position of the mirror pole is

$$r_{tan,0} = \frac{2}{sin\theta}\frac{R_0R_0'}{(R_0+R_0')} \tag{14}$$

Using Eqs. (13) and (14), we evaluated the desired ROC of the surface of the mirror under test at the mirror center in both the tangential and sagittal directions to be, respectively:

$$r_{tan,0} = 45.846 \text{ m} \quad \text{and} \quad r_{sag,0} = 55.839 \text{ m} \tag{15}$$

Using the CTRS procedure, we measured the sagittal slope variation by tracing the curvature along the sagittal direction at different positions along the tangential direction – Fig. 10.

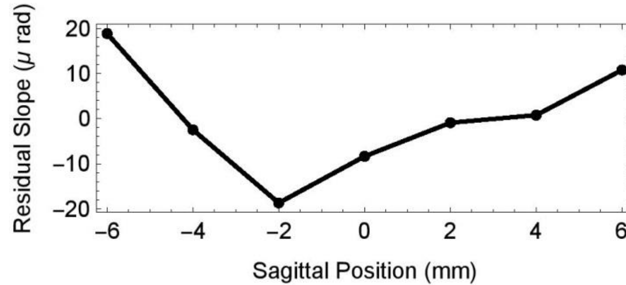

Figure 10. Residual slope variation of the 3D ellipsoidal mirror at the center tangential position found from integrated curvature traces as a function of sagittal position.

The central trace's detrended ROC was 55.915 mm. The sagittal ROC were measured for the CTRS method at five different tangential positions as a proof of principle for the developed measurement method and the correspondence between the measured shape and the analytical expression for the ideal spheroid. The residual sagittal slope variation measured at the center trance tangential position was 12.2 µrad (rms), and that is within the mirror specification.

4. DISCUSSION AND CONCLUSION

We have provided the mathematical foundation of the procedure for precision measurement of surface slope distributions of 3D x-ray mirrors significantly curved in the sagittal direction. We have demonstrated the efficacy of the method on the examples of measurements with three different mirrors with sagittal radius of curvature between 56 mm and 480 mm.

We have also presented an analytical expression describing the ideal surface shape in the sagittal direction of a spheroid specified by the conjugate parameters of the optic's beamline application. The expression was used for comparison of the measured slope distribution with the desired one.

4.1 Validity of residual slope trace via local curvature domain measurements

The theory of the CTRS method is based on a small angle approximation which says that the integral of curvature is approximately the slope. Groups from PTB and the University of Arizona have more in-depth discussions[29,30] on curvature stitching. Their curvature stitching method is for constructing the height map, when process of surface reconstruction is more complicated than our more basic slope reconstruction. Since the initial value of slope is unknown, this method is able to produce the residual sagittal slope of the surface of a mirror after removal of best first curvature.

4.2 Problems from aberrations and reexamining the extraction of curvature

The calibration of the NewView microscope was done by comparing curvature detrendings with the XROL DynaFiz interferometer, a subtle approximation invoked is that the aberrations of the objective lens are small. We plan to investigate the effects of these small aberrations on the curvature detrending values because they could be dependent on the mirror's curvature. Another aspect of the CTRS method that will be revised is the numerical integration step. In a basic numerical integral, the data points are not equally weighted which means the order of the data matters. There are more effective methods of integration that will potentially remove the issue of weighted data and return more accurate residual slope results. The long-term goal is to develop a system capable for reliable automatic measurements in the curvature domain.

ACKNOWLEDGEMENTS

The Advanced Light Source is supported by the Director, Office of Science, Office of Basic Energy Sciences, Material Science Division, of the U.S. Department of Energy under Contract No. DE-AC02-05CH11231 at Lawrence Berkeley National Laboratory.

This document was prepared as an account of work sponsored by the United States Government. While this document is believed to contain correct information, neither the United States Government nor any agency thereof, nor The Regents of the University of California, nor any of their employees, makes any warranty, express or implied, or assumes any legal responsibility for the accuracy, completeness, or usefulness of any information, apparatus, product, or process disclosed, or represents that its use would not infringe privately owned rights. Reference herein to any specific commercial product, process, or service by its trade name, trademark, manufacturer, or otherwise, does not necessarily constitute or imply its endorsement, recommendation, or favoring by the United States Government or any agency thereof, or The Regents of the University of California. The views and opinions of authors expressed herein do not necessarily state or reflect those of the United States Government or any agency thereof or The Regents of the University of California.

REFERENCES

[1] Yashchuk, V. V., Artemiev, N. A., Lacey, I., McKinney, W. R. and Padmore, H. A., “Advanced environmental control as a key component in the development of ultra-high accuracy ex situ metrology for x-ray optics,” Opt. Eng. 54(10), 104104/1-14 (2015); doi: 10.1117/1.OE.54.10.104104.

[2] Yashchuk, V. V., Artemiev, N. A., Lacey, I., McKinney, W. R. and Padmore, H. A., “A new X-ray optics laboratory (XROL) at the ALS: Mission, arrangement, metrology capabilities, performance, and future plans,” Proc. SPIE 9206, 92060I/1-19 (2014); doi:10.1117/12.2062042.

[3] Kirschman, J. L., Domning, E. E., McKinney, W. R., Morrison, G. Y., Smith, B. V., Yashchuk, V. V., "Performance of the upgraded LTP-II at the ALS optical metrology laboratory," Proc. SPIE 0770A-1 (2008).

[4] [4] McKinney, W. R., Anders, M., Barber, S. K., Domning, E. E., Lou, Y., Morrison, G. Y., Salmassi, F., Smith, B. V., Yashchuk, V. V., "Studies in optimal configuration of the LTP", Proc. SPIE 7801, 780106-11 (2010).

[5] Yashchuk, V. V., Barber, S., Domning, E. E., Kirschman, J. L., Morrison, G. Y., Smith, B. V., Siewert, F., Zeschke, T., Geckeler, R., Just, A., "Sub-microradian surface slope metrology with the ALS developmental long trace profiler," Nucl. Instr. and Meth. A 616, 212-223 (2010).

[6] Lacey, I., Artemiev, N. A., Domning, E. E., McKinney, W. R., Morrison, G. Y., Morton, S. A., Smith, B. V., and Yashchuk, V. V., “The developmental long trace profiler (DLTP) optimized for metrology of side-facing optics at the ALS,” Proc. SPIE 9206, 920603/1-11 (2014); doi:10.1117/12.2061969.

[7] Barber, S. K., Morrison, G. Y., Yashchuk, V. V., Gubarev, M. V., Geckeler, R. D., Buchheim, J., Siewert, F., Zeschke, T., “Developmental long profiler using optimally aligned mirror based pentaprism,” Opt. Eng. 50(5), 053601-1-10 (2011).

[8] Barber, S. K., Geckeler, R. D., Yashchuk, V. V., Gubarev, M. V., Buchheim, J., Siewert, F., Zeschke, T., “Optimal alignment of mirror based pentaprism for scanning deflectometric devices,” Opt. Eng. 50(7), 0073602-1-8 (2011).

[9] Siewert, F., Lammert, H., and Zeschke, T., “The nanometer optical component measuring machine,” in: Modern Developments in X-Ray and Neutron Optics, A. Erko, M. Idir, T. Krist, and A. G. Michette, Eds., Springer, New York (2008).

[10] Siewert, F., Buchheim, J., and Zeschke, T., “Characterization and calibration of 2nd generation slope measuring profiler,” Nucl. Instrum. Methods A 616(2-3), 119–127 (2010); http://doi.org/10.1016/j.nima.2009.12.033.

[11] Takacs, P. Z., Church, E. L., Bresloff, C. J., Assoufid, L., “Improvements in the accuracy and the repeatability of long trace profiler measurements,” Appl. Optics 38(25), 5468-5479 (1999).

[12] Takacs, P. Z., “X-ray optics metrology,” in: Handbook of Optics, 3rd ed., Vol. V, M. Bass, Ed., Chapter 46, McGraw-Hill, New York (2009).

[13] Alcock, S. G., Sawhney, K. J. S., Scott, S., Pedersen, U., Walton, R., Siewert, F., Zeschke, T., Senf, F., Noll, T., and Lammert, H., “The Diamond-NOM: A non-contact profiler capable of characterizing optical figure error with sub-nanometre repeatability,” Nucl. Inst. and Methods A 616(2-3), 224-228 (2010).

[14] Nicolas, J., Pedriera, P., Sics, I., Ramirez, C., and Campos, J., “Nanometer accuracy with continuous scans at the ALBA-NOM,” Proc. SPIE 9962, Advances in Metrology for X-Ray and EUV Optics VI, 996203 (2016); doi:10.1117/12.2238128.

[15] Qian, J., Sullivan, J., Erdmann, M., and Assoufid, L., “Performance of the APS optical slope measuring system,” Nucl. Instr. and Meth. A 710, 48-51 (2013); https://doi.org/10.1016/j.nima.2012.10.102.

[16] Qian, S., Geckeler, R., Just, A., Idir, M., and Wu, H., “Approaching sub-50 nanoradian measurements by reducing the saw-tooth deviation of the autocollimator in the Nano-Optic-Measuring Machine,” Nucl. Instr. and Meth. A 785, 206-212 (2015); doi: 10.1016/j.nima.2015.02.065.

[17] Yamauchi, K., Yamamura, K., Mimura, H., Sano, Y., Saito, A., Ueno, K., Endo, K., Suovorov, A., Yabashi, M., Tamasaku, K., Ishikawa, T., Mori, Y., "Microstitching interferometry for x-ray reflective optics," Rev. Sci. Instrum. 74, 2894-2898 (2003).
[18] Mimura, H., Yumoto, H., Matsuyama, S., Yamamura, K., Sano, Y., Ueno, K., Endo, K., Mori, Y., Yabashi, M., Tamasaku, K., Nishino, Y., Ishikawa, T., Yamauchi, K., "Relative angle determinable stitching interferometry for hard x-ray reflective optics," Rev. Sci. Instrum. 76, 045102 (2005).
[19] Kimura, T., Ohashi, H., Mimura, H., Yamakawa, D., Yumoto, H., Matsuyama, S., Tsumura, T., Okada, H., Masunaga, T., Senba, Y., Goto, S., Ishikawa, T., Yamauchi, K., "A stitching figure profiler of large X-ray mirrors using RADSI for subaperture data acquisition," Nucl. Instrum. Methods Phys. Res. A 616, 229-232 (2010).
[20] Yamauchi, K., Mimura, H., Kimura, T., Yumoto, H., Handa, S., Matsuyama, S., Arima, K., Sano, Y., Yamamura, K., Inagaki, K., Nakamori, H., Kim, J., Tamasaku, K., Nishino, Y., Yabashi, M., and Ishikawa, T., "Single-nanometer focusing of hard x-rays by Kirkpatrick–Baez mirrors," J. Phys.: Condens. Mattter. 23(39), 394206 (2011); https://doi.org/10.1088/0953-8984/23/39/394206.
[21] Yaroslavsky, L. P., Moreno, A., Campos, J., "Frequency responses and resolving power of numerical integration of sampled data," Optics Express 2892-2905 (2005).
[22] Lacey, I., Artemiev, N. A., McKinney, W. R., Merthe, D. J., Yashchuk, V. V., "High precision surface metrology of x-ray optics with an interferometric microscope," Proc. SPIE 8838, 883808 (2013).
[23] Polonska, K. S., Gevorkyan, G. S., Yashchuk, V. V., "Measurements with ZYGO NewView-7300 interferometric microscope of the tangential radius of curvature, surface slope variation and the roughness of a highly curved glass sample," LSBL Note LSBL-1296 (2016).
[24] Centers, G., Yashchuk, V. V., "Measurements with ZYGO NewView-7300 interferometric microscope of the sagittal radius of curvature, sagittal slope variation, and surface roughness of BL 5.3.2.2 Toroidal Mirror 5315-100," LSBL Note LSBL-1278 (Berkeley, 2015); available upon request.
[25] Yashchuk, V. V., Centers, G., "ZYGO NewView-7300 interferometric microscope measurements with the M124 ellipsoid mirror for the ALS BL 8.0.1.2," LSBL Note LSBL-1286 (Berkeley, 2016); available upon request.
[26] Yashchuk, V. V., "Optimal measurement strategies for effective suppression of drift errors," Rev. Sci. Instrum. 80, 115101 (2009).
[27] Ali, Z., Artemiev, N. A., Cummings, C. L., Domning, E. E., Kelez, N., McKinney, W. R., Merthe, D. J., Morrison, G. Y., Smith, B. V., Yashchuk, V., "Automated suppression of errors in LTP-II slope measurements with x-ray optics," Proc. SPIE 7141, 81410O (2011).
[28] Yashchuk, V. V., Centers, G., "Ellipsoid of revolution (Spheroid): Basic equations," LSBL Note LSBL-1283 (Berkeley, 2016); available upon request.
[29] Elster, C., Gerhardt, J., Schmidt, P. T., Schulz, M., Weingartner, I., "Reconstructing surface profiles from curvature measurements,"Optik Optics 113, 154-158 (2002).
[30] Kim, D. W., Kim, B. C., Zhao, C., Oh, C. J., Burge, J. H., "Algorithms for surface reconstruction from curvature data for freeform aspherics," Proc. SPIE 8838, 88380B-1 (2013).